



# Numerical Evaluation of the Axial Resistance Force in Steel Column Design

Alexandre Rossi<sup>1</sup>, Felipe Piana Vendramell Ferreira<sup>1</sup>  
and Carlos Humberto Martins<sup>1\*</sup>

<sup>1</sup>Department of Civil Engineering, State University of Maringá, Maringá – PR, Brazil.

## Authors' contributions

*This work was carried out in collaboration between all authors. The authors AR and FPVF designed the study, performed the numerical analysis, wrote the protocol, and wrote the first draft of the manuscript. Author CHM managed the analyses of the study. All authors managed the literature searches. All authors read and approved the final manuscript.*

## Article Information

DOI: 10.9734/CJAST/2017/38210

### Editor(s):

(1) João Miguel Dias, Assistant Professor, Habilitation in Department of Physics, CESAM, University of Aveiro, Portugal.

### Reviewers:

(1) Shashidhar K. Kudari, CVR College of Engineering, JNT University, India.

(2) G. Y. Sheu, Chang-Jung Christian University, Taiwan.

(3) Yong Gan, California State Polytechnic University, USA.

Complete Peer review History: <http://www.sciencedomain.org/review-history/22214>

**Original Research Article**

**Received 17<sup>th</sup> November 2017**

**Accepted 4<sup>th</sup> December 2017**

**Published 8<sup>th</sup> December 2017**

## ABSTRACT

The finite element method (FEM) is a form of computational analysis that provides approximated results with acceptable accuracy. By using the FEM, developing theoretical models capable of properly analyzing the effects of the structural behavior under the influence of proposed imperfections becomes easier and more economical. Metal columns are elements that, when subjected to axial compressive forces, undergo a phenomenon called buckling. This phenomenon consists of the loss of stability in the element, causing a displacement in the buckling axis of the structure. However, some construction imperfections in the materials cause the buckling phenomenon to not have the classic behavior predicted in the studies by Euler. Therefore, this study will present a numerical analysis of metal columns in rolled profiles with parallel flanges. During the simulations, the variations in physical and geometrical imperfections were evaluated with different distribution models. The purpose was to evaluate the influence of such imperfections on flexural buckling, comparing the results obtained with numerical simulations to those obtained analytically. As indicated by the results of this evaluation, the physical

\*Corresponding author: E-mail: [chmartins2007@gmail.com](mailto:chmartins2007@gmail.com);

and geometrical imperfections influence buckling in the case of columns with low slenderness ratios, significantly decreasing their strength. For higher slenderness ratios, i.e., greater lengths, this effect is decreased.

*Keywords: Buckling; imperfections; residual stress; axial force.*

## 1. INTRODUCTION

Metal columns used in civil construction are usually profiles with parallel flanges. These profiles are manufactured at high temperatures in metallurgical plants; one such manufacturing process is known as rolling, a process that is responsible for the presence of physical and geometrical imperfections. Fig. 1 shows the distribution of residual stresses in a rolled profile, in this case the value of the residual compressive ( $\sigma_{rc}$ ) stress is taken as 0.3 of the yield stress of steel ( $f_y$ ).

According to Beck and Dória [1], the compressive strength of steel columns depends on physical and geometrical properties, such as the geometrical cross section, slenderness, modulus of elasticity, residual stresses, and geometrical imperfections.

### 1.1 Buckling

The required condition for a structure (beam, pillar, etc.) to behave properly during its service life is to not reach the so-called limit states, i.e., the states in which the structure will stop providing its designed functions. There are two types of limit states: the ultimate limit state and the serviceability limit state. The serviceability limit state is related to the economical use and the integrity of materials supported by the structure, as well as the comfort of users. In turn, the ultimate limit state is associated with the partial or total collapse of a structure due to the depletion of the bearing capacity of the structure.

In metal columns, as observed in Fig. 2, the ultimate limit states due to bending are generally associated with one of the following factors: the total or partial yielding of one or more cross sections (formation of plastic hinges), the flange local buckling and the web local buckling. As can be observed in Fig. 2 for long columns, which have a high slenderness index ( $\lambda$ ), buckling occurs in the elastic phase, where the observed stresses are lower than the yield stress of steel

( $\sigma_e$ ). For columns of intermediate length, slenderness upper to slenderness of plastification ( $\lambda_{im}$ ) and less than slenderness of elastic buckling ( $\lambda_n$ ), buckling occurs in the inelastic phase where some regions of plastification can be observed, because tensions higher than the yield stress of steel are observed. Finally, it is observed that for short columns, slenderness downward the plastification limit ( $\lambda_{im}$ ), the ultimate strength is given by the steel's own plastification stress ( $\sigma_p$ ), with no buckling occurring, but the total plastification of the section. Theoretically, when an axial load  $P$  is increased until the occurrence of failure by fracture or yielding, i.e., when the critical load  $P_{cr}$  is reached, the column is at the limit of its stability. Therefore, if a small lateral force  $F$  is removed, the column will remain at the flexed position. Any reduction in  $P$  to a value lower than  $P_{cr}$  causes the column to remain straight, and any increase in  $P$  higher than  $P_{cr}$  causes a greater lateral deflection, fact that characterizes the phenomenon of buckling. The ability of the column to restore itself is based on its flexural strength.

### 1.2 Physical and Geometrical Imperfections

According Wang, Li and Chen [3] the physical imperfections, i.e., the residual stresses, appear in structural profiles and steel plates during the manufacturing process and will inevitably remain there unless stress relief techniques are used. During the non-uniform cooling, after rolling or welding the part, plastic deformations and therefore residual stresses occur, which in some cases could reach the same magnitude of the material's yield strength. The residual stresses have an important role in the design of the steel pillars. Because they are the main cause for the nonlinearity of the stress-strain diagram in the inelastic region, according to Alpsten and Tall [4], they significantly affect the compressive strength.

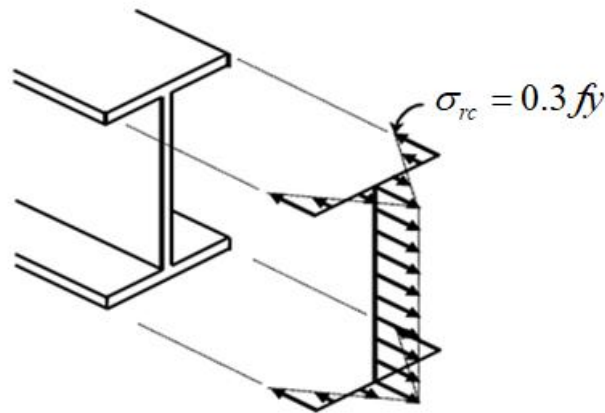


Fig. 1. Rolled profile (I-beam) with residual stresses – Ref. [1]

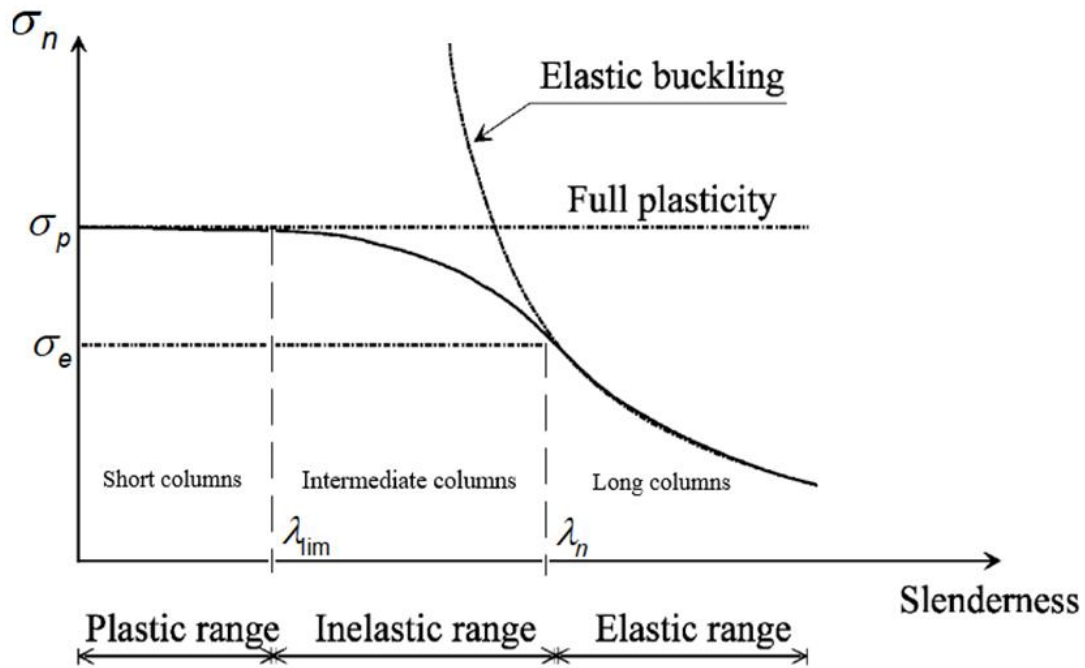


Fig. 2. Buckling intervals in metal columns – Adapted from Ref. [2]

The residual stresses represent a state of self-equilibrating internal stresses in the steel profiles as a result of the industrial production processes. They occur in bodies that undergo non-uniform plastic deformations. If no external forces oppose them, residual stresses will always be elastic. The non-homogeneous deformation condition, which creates the residual stresses in the steel sections, is due to the thermal (rolling, welding and flame cutting) and mechanical industrial processes (cold rolling and straightening).

In hot-rolled profiles, the residual stress formation process causes the extremities of the flanges and the center section of the web to be compressed, whereas the joints between the web and the flange are in tension due to the slow cooling. For profiles welded with universal mill plates, the weld that joins the flanges to the web induces residual compressive stresses on the extremities of the flanges, expanding the region of residual compressive stresses and adversely affecting the strength of pillars compared to pillars composed of hot-rolled profiles. In the profiles welded with flame-cut plates, the cut

introduces tensile stresses in the edges of the plates due to the heat, which has a favorable effect on the compressive strength (Bjorhovde & Tall [5]; Mc Falls & Tall [6]; ECCS [7], Szalai & Papp [8], Spoorenberg, Snijder and Hoenderkamp [9]).

The technical literature has adopted simplified forms of the parabolic or linear distributions for the residual stress variations of rolled and welded profiles. Many authors (Kanchanalai [10]; Chen & Toma [11]; Chen et al.; Kim & Chen [12, 13], among others) use the linear distribution in the flanges and the constant distribution in the web in analysis models that consider the residual stresses. Nevertheless, for profiles with long webs, the stress variations along the web should also be considered. Hence, a good approximation would be to consider parabolic or linear distributions for both the flanges and the web.

The functioning of structures composed of rolled, welded or cut steel profiles, such as metal pillars, primarily depends on the residual stresses that they present.

In turn, the presence of geometrical imperfections in the columns, such as the initial curvature, transforms the buckling problem into a load-displacement problem, which opposes the problem of bifurcation of the equilibrium. According to Galambos [14,15], the real configuration of the initial curvature of a pillar may vary a lot and can present simple, double, or reverse curvatures or even curvatures in the two primary directions of the profile cross section (ECCS [7]). Additionally, the amplitude of the initial imperfections could vary widely along the pillar.

Therefore, the objective is to evaluate the effects of these imperfections during the buckling process of the columns constituted by H-shaped profiles. Through the variation of the physical and geometric imperfection models, the critical situation is determined, that is, the provides the least resistance. The numerical analysis results are also compared with the Euler proposal and ABNT NBR 8,800: 2008 [16].

## 2. CALCULATION METHODS

The Brazilian norm of reference ABNT NBR 8,800:2008 [16] (Design and Execution of Steel structures in Buildings – Limit States Method)

establishes a method for calculating the axial resistance force, found in item 5.3.2 of the norm.

The design axial compressive strength of a structure,  $N_{c,Rd}$ , which is associated with the ultimate limit states of instability by bending, torsion or flexural-torsion and local buckling, should be determined by Eq. (1):

$$N_{c,Rd} = \frac{\chi Q A_g f_y}{\gamma_{a1}} \quad (1)$$

where:

$\chi$  is the reduction factor associated with the compressive strength;

$Q$  is the total reduction factor associated with local buckling;

$f_y$  is the yield stress of the steel;

$A_g$  is the gross cross section area of the beam; and

$\gamma_{a1}$  is the weighted strength coefficient.

For the calculation according to ABNT NBR 8,800:

- ASTM A572 Steel,  $f_y = 34.5 \text{ kN/cm}^2$ , the ultimate tension of the steel is  $f_u = 45.0 \text{ kN/cm}^2$ ; and
- I-beam with double-symmetric cross sections.

According to table F-1 of annex F from ABNT NBR 8,800:2008 [15], the I-beam web belongs to group AA 2 because the web is the supported-supported element of section I. The flanges belong to group AL 4 because they fit the profile of the group of supported-free elements of section I. Therefore, the total reduction factor associated with the local buckling will be given by Eq. (2):

$$Q = Q_a Q_s \quad (2)$$

where:  $Q_a$  and  $Q_s$  are reduction factors that take into account the local buckling of the elements

However, because in both the web and the flange the width/thickness ( $b/t$ ) ratio is smaller than  $b/t_{lim}$ , the reduction factor will be given by Eq. (3):

$$Q = 1 \quad (3)$$

According to annex E of ABNT NBR 8,800:2008 [15], for double-symmetric cross sections, such as that of I-beams, the elastic axial buckling stress ( $N_e$ ) is given by Eq. (4):

$$N_{ey} = \frac{\pi^2 E I_y}{(k_y L_y)^2} \quad (4)$$

where:

- $E$  is the elasticity modulus of steel;
- $I_y$  is the moment of inertia about the y-axis;
- $k_y$  is the coefficient of the buckling length; and
- $L_y$  is the buckling length in the y-direction.

After performing the calculations above, the value of the reduction coefficient associated with the compressive strength ( $\chi$ ) is determined by Eqs. (5) and (6):

$$\lambda_0 \leq 1.5 \text{ SO } \chi = 0.658^{\lambda_0^2} \quad (5)$$

$$\lambda_0 > 1.5 \text{ SO } \chi = \frac{0.877}{\lambda_0^2} \quad (6)$$

Where ( $\lambda_0$ ) is given by Eq. (7):

$$\lambda_0 = \sqrt{\frac{Q A_g f_y}{N_e}} \quad (7)$$

Hence, the design axial resistance force can be calculated ( $N_{c,Rd}$ )

### 3. NUMERICAL ANALYSIS

The numerical analyses were developed with the ABAQUS 6.12 Software [17], which uses the Finite Element Method (FEM). For the discretization of the numerical model, shell elements of type S4R with a width of 20 mm were used. Four nodes, six degrees of freedom per node and reduced integration characterize this element. This reduced integration is responsible for an increase in the quality of the results in relation to the displacements and the reduction in the time of analysis. The Fig. 3 shows the element used and the discretized model.

Initially, elastic buckling analyses were performed using the buckling calculation model, a procedure for linear perturbation analysis of eigenvalues and eigenvectors, where the first eigenvalue, the elastic buckling load factor and its respective eigenvector determine the deformation. Then, in the post-buckling analysis for the application of the physical and geometrical imperfections, the Static Riks calculation method was applied, which is generally used to prevent structural collapse and is extensively used in nonlinear physical and geometrical analyses. This calculation method applies the eigenvalue of the buckling analysis to provide complete information on the structural collapse. Additionally, it is especially used to increase the rate of convergence of the method due to instability issues.

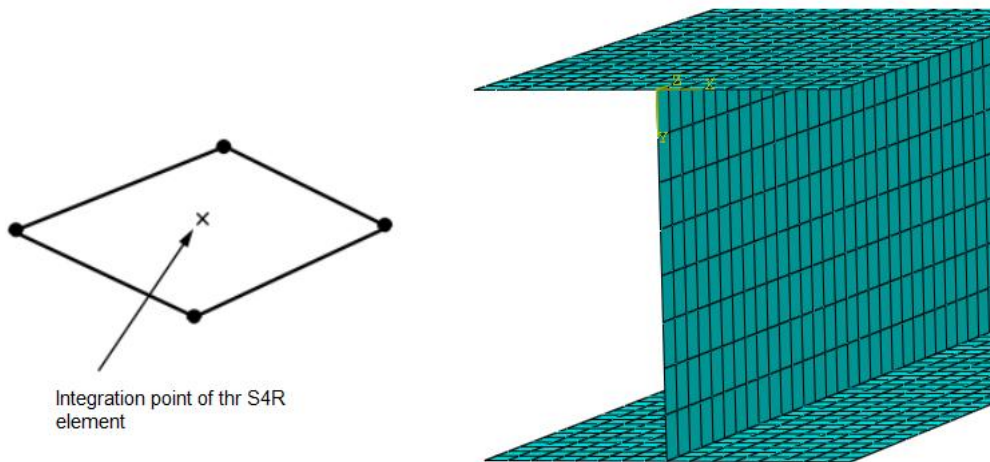


Fig. 3. Representation of the S4R element and the discretized model

The metal columns were simulated with the HP 250x85 profile, GERDAU AÇOMINAS standard, with boundary conditions of a pinned-pinned pillar. Therefore, the buckling length ( $L_b$ ) is equal to the actual length, with slenderness ratios of 20, 40, 60, 80, 100, 120, 140, 160, 180, 200, 215 and 225. The selected ASTM A36 steel, grade 50, has a modulus of elasticity of  $E = 20,000 \text{ kN/cm}^2$  and a yield stress of  $f_y = 34.5 \text{ kN/cm}^2$ . The value for the maximum residual compressive stress was adopted according to ABNT NBR 8,800:2008 [15]. The load was gradually increased from 0.5% up to the normal yield strength for the cross section in the centered compression of the beam,  $P_y = Af_y = 3,581.93 \text{ kN}$ , where  $A$  represents the total cross-sectional area of the column and  $f_y$  the yield stress of the steel. This load was distributed along the entire beam cross section in the z-direction to avoid yielding problems in the location where the load is applied.

To perform the simulation of the models under the influence of geometrical imperfections (initial curvature), the following geometrical imperfection values were used:  $L/300$ ,  $L/500$ ,  $L/750$ ,

$L/1,000$ ,  $L/1,500$ ,  $L/2,000$  and  $L/4,000$ , where  $L$  represents the unlocked length of the column. For the physical imperfections, five models were used, as shown in Table 1.

#### 4. RESULTS

The analyses were performed with the initial considerations of physical and geometrical imperfections separately. In the first case, simulations of the physical imperfections were performed by varying the models according to Table 1, as shown in Fig. 4. Then, the simulations of the models of geometrical imperfections were performed, as previously presented and the results are shown in Fig. 5. Finally, the imperfections were combined, generating a model with both physical and geometrical imperfections, therefore Fig. 6 presents the results for the columns analyzed with the combination of the five residual stress models presented in Table 1 with a geometric imperfection of  $L/1,000$ . This value of geometric imperfection was adopted because it is the maximum tolerated value in structural profiles (Kala and Valeš [18], Bjorhovde [19]).

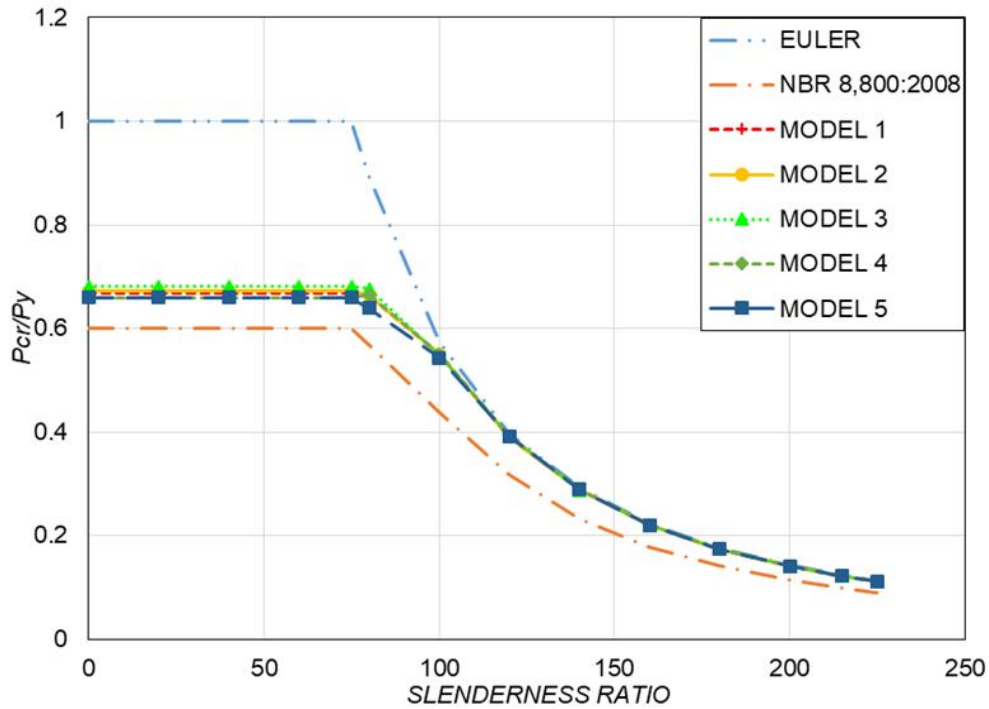


Fig. 4.  $\lambda$  versus  $P_{cr} / P_y$  curves for different models of physical imperfections

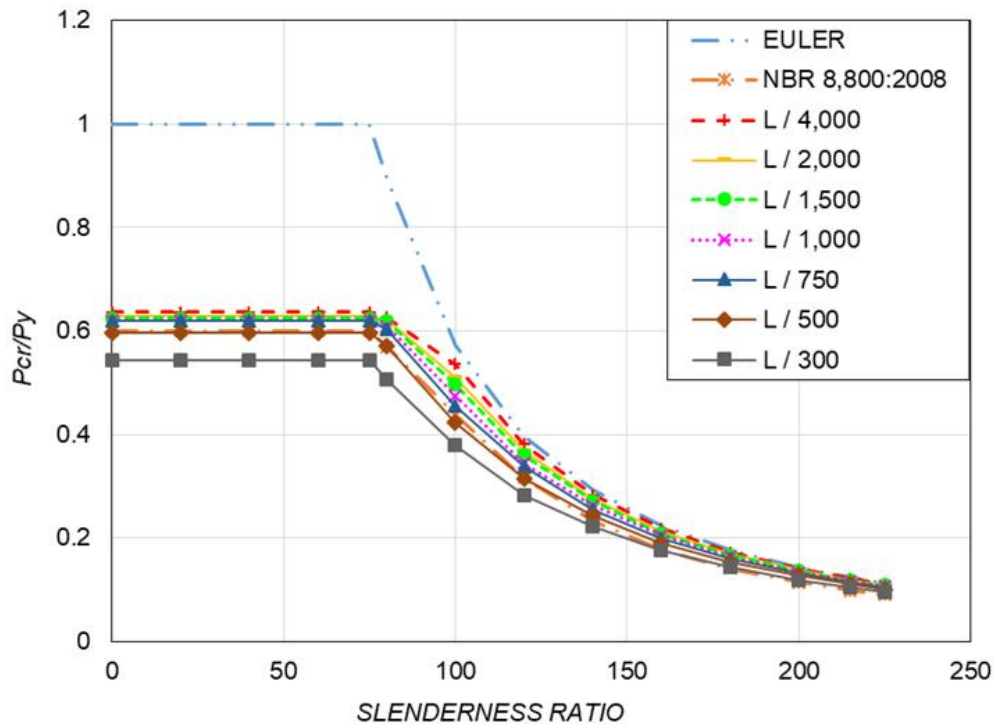


Fig. 5.  $\lambda$  versus  $P_{cr} / P_y$  curves for different models of geometrical imperfections

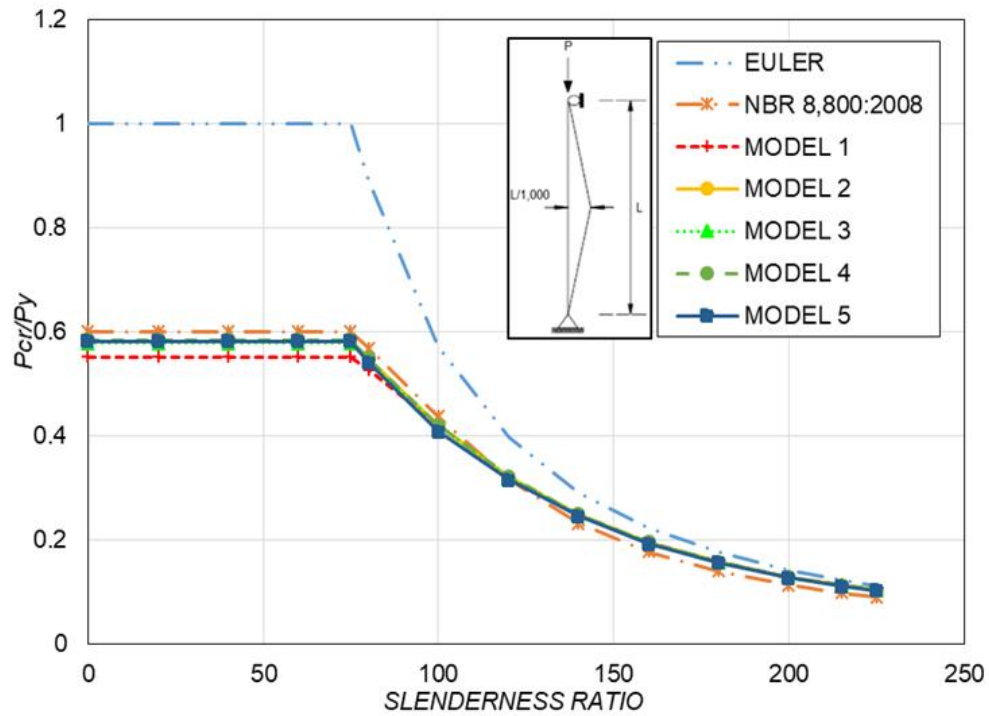
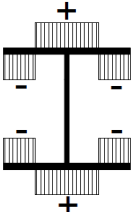

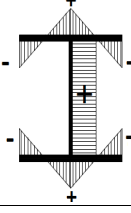
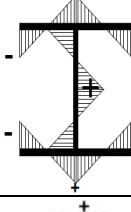
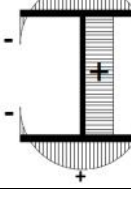


Fig. 6.  $\lambda$  versus  $P_{cr} / P_y$  curves for different models of physical and geometrical imperfections with a geometrical imperfection of  $L/1,000$

**Table 1. Models of physical imperfections**

Setup	Distribution		Residual tensile stress ( $\sigma_{rt}$ )	Model
	Flange	Web		
	Constant	Without	$\sigma_{rt} = -\sigma_{rc}$	1
	Linear	Without	$\sigma_{rt} = -\sigma_{rc}$	2
	Linear	Constant	$\sigma_{rt} = \frac{t_f b_f}{t_f b_f + t_w d_w} \sigma_{rc}$ Onde: $d_w = d - 2t_f$	3
	Linear	Linear	$\sigma_{rt} = -\sigma_{rc}$	4
	Linear	Constant	$\sigma_{rt} = \frac{2t_f b_f}{4t_f b_f + 3t_w d_w} \sigma_{rc}$	5

Therefore, the following results relate the ratio between the critical buckling load ( $P_{cr}$ ) and the yield load of the section ( $P_y$ ) to the different slenderness ratios of the column, which has the HP250x85 profile as the geometrical section. This profile was selected because HP profiles are the most commonly used profile for metal columns. In the Fig. 4, 5 e 6 are presented the results of the analysis of the columns constituted by the profile HP250x85.

The results presented in Figs. 4, 5 and 6 show that the buckling curves obtained in the

numerical analyzes under the application of imperfections presented a considerable difference when compared with the Euler curve for values of slenderness less than 75. This difference was due to the fact that plastification of the geometric section occurs for values of slenderness less than 75 for the numerical analyzes carried out, where the critical load is still much lower than the plastification load, due to the effect of the physical and geometrical imperfections, a situation that is not observed in the buckling curve of Euler.



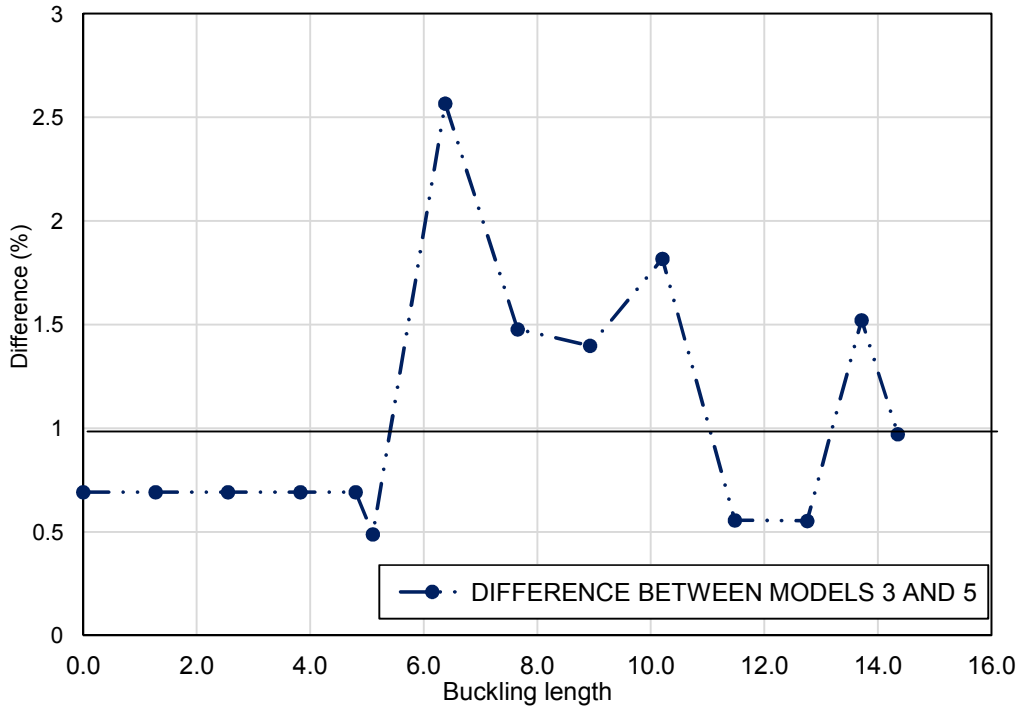


Fig. 7. Difference between models 3 and 5 of physical imperfections for profile HP250x85

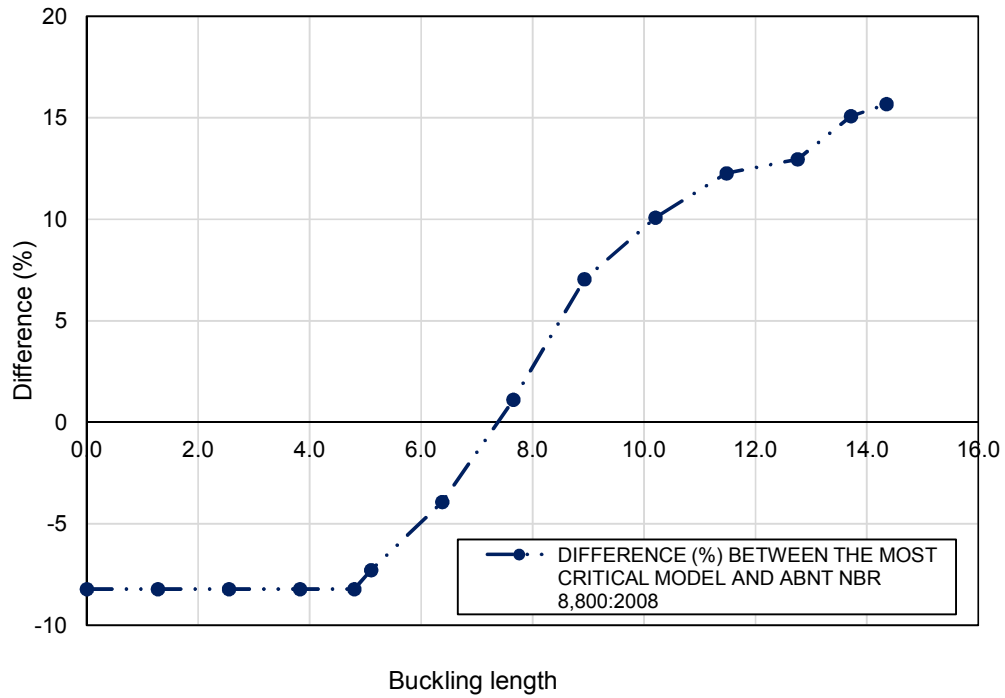


Fig. 8. Difference between the model with the combination of imperfections and ABNT NBR 8,800:2008

## 5. CONCLUSION

According to the results from the analyses of a HP250x85 beam, the variation in the buckling load was small for the different models of physical imperfections, i.e., regardless of the distribution of the residual stresses in the metal profiles, the results were similar. This can be observed in the Fig. 7, which shows the difference between the residual stress models that presented the largest variation in profile HP250x85.

It was also observed that the ABNT NBR 8,800:2008 [16] calculation method is conservative in relation to the physical imperfections, and for all of the studied models, the results exhibited higher values than those obtained by the calculations according to this standard.

The results of the models only containing the geometrical imperfections presented a large variation, i.e., the geometrical imperfection is a more determinant factor in the reduction of the buckling load, and for lower values, the reduction is much more significant. The ABNT NBR 8,800:2008 [16] calculation method proved to be conservative in relation to most of the models. Additionally, it was possible to conclude that the standard loses its effectiveness for geometrical imperfection values larger than  $L/500$ .

In turn, when the physical and geometrical imperfections are combined, there is a concerning result in relation to the calculation model provided by ABNT NBR 8,800:2008. In contrast to the elastic buckling phase, where all imperfection models – combined or not – were superior to the norm, i.e., where the norm is conservative, the norm did not have the same behavior in the inelastic and plastic buckling phases. For all combined models of physical and geometrical imperfections, the norm proved to be deficient, where the values found for the buckling load were lower than that calculated according to the norm. This can be observed in the Fig.8 for the most critical model observed in profile HP 250x85: the combination of the physical imperfection model 1 and a geometrical imperfection of  $L/1,000$ .

Therefore, it is concluded that the combination of the physical and geometrical imperfections should be an important factor to consider in structural calculations, especially when the structure is designed in the inelastic or plastic

buckling phase because, as observed in Fig. 8 for profile HP 250x85, for lengths smaller than 7.4 m, the resistance value is lower than that calculated with ABNT NBR 8,800:2008.

## COMPETING INTERESTS

Authors have declared that no competing interests exist.

## REFERENCES

1. Beck AT, Dória AS. Reliability analysis of I-section steel columns designed according to new Brazilian building codes. *Journal Of The Brazilian Society Of Mechanical Sciences And Engineering*, [s.l.]. 2008;30(2):152-159.
2. Vila Real PMM, Cazeli R, Silva IS, Santiago A, Piloto P. The effect of residual stresses in the lateral torsional buckling of steel I-beams at elevated temperature. *Journal of Constructional Steel Research*. 2004;60:783-793.
3. WANG, Yan-bo LI, Guo-qiang CHEN, Su-wen. Residual stresses in welded flame-cut high strength steel H-sections. *Journal of Constructional Steel Research*, [s.l.]. 2012;79:159-165,
4. Alpsten GA, Tall L. Residual stresses in heavy welded shapes. *Welding Journal/ AWS*. 1970;93-105.
5. Bjorhovde R, Brozzetti J, Alpsten GA, Tall L. Residual stresses in thick welded plates. *Welding Journal (AWS)*. 1972;51:329-405.
6. MC Falls RK, Tall L. A study of welded columns manufactured from flame-cut plates. *Welding Journal/ AWS*. 1969;141-153.
7. ECCS. Manual on the stability of steel structures – European Convention for Constructional Steelwork (ECCS). 2° ed., Brussels; 1976.
8. Szalai JE, PAPP F. A new residual stress distribution for hot-rolled I-shaped sections. *Journal of Constructional Steel Research*. 2005;61:845-861.
9. Spoorenberg RC, Snijder HH, Hoenderkamp JCF. Experimental investigation of residual stresses in roller bent wide flange steel sections. *Journal of Constructional Steel Research*. 2010;66: 737-747.
10. Kanchanalai T. The design and behavior of beam-columns in Unbraced Steel Frames. *AISI Project N°. 189, Report N°. 2,*

- Civil Engineering/Structures Research Laboratory, University of Texas, Austin (TX). 1977;300.
11. Chen WF, Goto Y, Liew JYR. Stability design of semi-rigid frames. New York: John Wiley e Sons, Inc. 1996;468.
  12. Kim SE, Chen WF. Practical advanced analysis for braced steel frame design. Journal of Structural Engineering, ASCE. 1996a;122(11):1266-1274.
  13. Kim SE, Chen WF. Practical advanced analysis for braced steel frame design. Journal of Structural Engineering. 1996b;122(11):1259-1265.
  14. Galambos TV. Guide to stability design criteria for metal structures, 4<sup>th</sup> Ed., A. Wiley – Interscience; 1988.
  15. Galambos TV, Surovek AE. Structural stability of steel: Concepts and applications for structural engineers. 1<sup>o</sup> edição. Hoboken, New Jersey: John Wiley & Sons; 2008.
  16. Associação brasileira de normas técnicas. ABNT NBR 8800: Projeto e execução de estruturas de Aço de Edifícios – Métodos dos Estados Limites, Rio de Janeiro; 2008.
  17. Dassault Systèmes. Abaqus. 2011;6.12.
  18. Kala Z, Valeš J. Global sensitivity analysis of lateral-torsional buckling resistance based on finite element simulations. Engineering Structures. 2017;134:37-47.
  19. Bjorhovde R. Columns: From theory to practice. Engineering Journal (AISC). 1988;25(1):21-34.

© 2017 Rossi et al.; This is an Open Access article distributed under the terms of the Creative Commons Attribution License (<http://creativecommons.org/licenses/by/4.0>), which permits unrestricted use, distribution, and reproduction in any medium, provided the original work is properly cited.

*Peer-review history:*  
*The peer review history for this paper can be accessed here:*  
<http://sciencedomain.org/review-history/22214>